

---

# GLEO-DET: DEEP CONVOLUTION FEATURE-GUIDED DETECTOR WITH LOCAL ENTROPY OPTIMIZATION FOR SALIENT POINTS

---

A PREPRINT

✉ **Chao Li**

School of Artificial Intelligence  
Beijing University of Posts and Telecommunications  
chaoli@bupt.edu.cn

✉ **Yanan You\***

School of Artificial Intelligence  
Beijing University of Posts and Telecommunications  
youyanan@bupt.edu.cn

**Wenli Zhou**

School of Artificial Intelligence  
Beijing University of Posts and Telecommunications  
zwl@bupt.edu.cn

April 28, 2022

## ABSTRACT

Feature detection is an important procedure for image matching, where unsupervised feature detection methods are the detection approaches that have been mostly studied recently, including the ones that are based on repeatability requirement to define loss functions, and the ones that attempt to use descriptor matching to drive the optimization of the pipelines. For the former type, mean square error (MSE) is usually used which cannot provide strong constraint for training and can make the model easy to be stuck into the collapsed solution. For the later one, due to the down sampling operation and the expansion of receptive fields, the details can be lost for local descriptors can be lost, making the constraint not fine enough. Considering the issues above, we propose to combine both ideas, which including three aspects. 1) We propose to achieve fine constraint based on the requirement of repeatability while coarse constraint with guidance of deep convolution features. 2) To address the issue that optimization with MSE is limited, entropy-based cost function is utilized, both soft cross-entropy and self-information. 3) With the guidance of convolution features, we define the cost function from both positive and negative sides. Finally, we study the effect of each modification proposed and experiments demonstrate that our method achieves competitive results over the state-of-the-art approaches.

**Keywords** Feature detection · Image matching · Entropy · Guidance

## 1 Introduction

Matching salient features across images is an essential premise in many computer vision tasks, such as 3D reconstruction, visual localization and image retrieval. In order to find the local areas that can be matched, one essential premise is to find the salient features with rich semantic information, which is quite crucial in the entire image matching procedure.

Earlier studies mostly concentrate on corner features and blob features, which are of the handcrafted methods based on the expert knowledge. Corner features are usually extracted based on the gradient, intensity or curvature information, among which the first two are more frequently applied, for instance, Harris [Harris et al., 1988], SUSAN [Smith and Brady, 1997], FAST [Trajković and Hedley, 1998], ORB [Rublee et al., 2011] and AGAST [Mair et al., 2010]. Different

---

\*Corresponding author.

from the corner features, a blob feature generally contains the blob shape information, including scale and orientation. Classical blob features can be generated based on second-order partial derivative and segmentation, such as Laplacian of Gaussian (LoG) [Lindeberg, 1998], difference of Gaussian (DoG) [Lowe, 1999, 2004], SIFT [Lowe, 1999, 2004], SURF Bay et al. [2006] and MSER [Matas et al., 2004].

Intuitively, on the one hand, features with rich semantic information are more than just handcrafted ones, on the other hand, some of the handcrafted features may contain little semantic information. With the application of the convolution neural networks (CNN) [LeCun et al., 1998] in image processing, learning-based pipelines for feature detection have been studied in recent years. Supervised approaches like LIFT [Yi et al., 2016] and TILDE [Verdie et al., 2015] select the prominent handcrafted features as positive samples and the smooth areas as the negative samples to train the network. Self-supervised methods involves SuperPoint [DeTone et al., 2018], which firstly trains the MagicPoint [DeTone et al., 2018] based on simulated data set and then generates pseudo labels for further training. Unsupervised pattern is the one that has been studied most, including the ones that are based on repeatability requirement like LF-Net [Ono et al., 2018], RF-Net [Shen et al., 2019], UnsuperPoint [Christiansen et al., 2019] and Key.Net [Barroso-Laguna et al., 2019], and the ones that use descriptor matching to drive the optimization of the detector such as D2-Net [Dusmanu et al., 2019], R2D2 [Revaud et al., 2019], and ASLFeat [Luo et al., 2020].

However, for the methods that leverage the feature repeatability and use MSE cost function when training, including LF-Net [Ono et al., 2018], RF-Net [Shen et al., 2019], UnsuperPoint [Christiansen et al., 2019] and Key.Net [Barroso-Laguna et al., 2019], constraint is weak and the model can be stuck into collapsed solution, making convergence difficult. While for the approaches that use local features to drive the learning of feature detector and train the descriptor and detector jointly, such as D2-Net [Dusmanu et al., 2019], R2D2 [Revaud et al., 2019] and ASLFeat [Luo et al., 2020], the constraint for detector is not fine enough due to down sampling operation and expansion of the receptive fields.

For the issue mentioned above, our contributions can be illustrated from three aspects. First, fine constraint is achieved via repeatability cost function while coarse constraint is realized with the guidance of convolution features. Second, to address the issue that optimization via MSE is limited for detection learning, we trained the detector with entropy-based loss function, making convergence easier. Third, we define cost function from both positive and negative sides under the guidance of convolution features, which aims to reject the key points with little semantic information. Eventually, our method shows good repeatability and mean matching accuracy, which illustrates that our method is not only precise for feature localization but also robust for matching.

## 2 Related Works

Detected features are special structures which represent certain semantic information in images, including corner features, blob features, edges and morphological region features. The most popular features used for image matching are key points. Good key point detection algorithm should be (i) stable and (ii) matchable. In other words, on the one hand, key points detected should be invariant to both illumination changes and spatial transform. on the other hand, they should also be rich in semantic information so that can be matched.

### 2.1 Handcrafted features

The most common handcrafted features used are corner features and blob features. A corner feature is a the cross point of two lines, which can be depicted in the form of "L", "T" and "X". To find out the corner features in an image, one approach is to leverage the gradient information, like Harris [Harris et al., 1988], and the other is to detect via intensity information directly, including SUSAN [Smith and Brady, 1997], FAST [Trajković and Hedley, 1998] and ORB [Rublee et al., 2011]. On the contrary, a blob feature is regarded as a closed region with not only the feature location information  $(x, y)$  but also the blob shape information  $(s, \theta)$ , indicating scale and orientation. Typical blob features involve classic Laplacian of LoG [Lindeberg, 1998], DoG [Lowe, 1999, 2004], SIFT [Lowe, 1999, 2004], etc.

Harris [Harris et al., 1988] firstly calculates the auto-correlation matrix with the gradient information for each location, and then finds the directions of the fastest and lowest grey-value changes to determine whether it is the key point. SUSAN [Smith and Brady, 1997] assumes a pixel as a key point when the intensity values of enough pixels in its neighboring area are different, and the distance between the centroid of the neighboring area and the pixel is far enough. FAST [Trajković and Hedley, 1998] takes comparison with intensity values of each pixel on a circle, and selects corner features using a machine learning approach trained on a large number of similar scene images. ORB [Rublee et al., 2011] uses the Harris [Harris et al., 1988] response to select FAST [Trajković and Hedley, 1998] key points as the final detected features.

Generally, the corner detection algorithms mentioned above are rotation-invariant but not scale-invariant without taking sale into consideration. Nevertheless, blob features are quite differnt. LoG [Lindeberg, 1998] determines blob features

through detecting local extremums on images convolved by scale-normalized Laplacian of Gaussian under different scales defined with the standard deviation  $\sigma$ . DoG [Lowe, 1999, 2004] is an improved version of scale-normalized LoG as they are approximately equal, which is more efficient. SIFT [Lowe, 1999, 2004] firstly constructs the DoG scale space and detects local extremums to obtain feature locations as well as scales. Subsequently, through the gradient histogram it calculates the directions for each key point. SIFT is a stable feature detection algorithm that has been widespread used in numerous tasks. Compared to the corner features above, blob features are usually both rotation-invariant as well as scale-invariant via using different  $\sigma$ s as scales.

## 2.2 Learning-based features

One issue for conventional handcrafted features like corners and blobs is that these features might not contain enough semantic information for matching in some cases. And numerous studies attempt to apply deep learning approaches to feature detection, in both supervised, self-supervised and unsupervised manners.

Supervised detectors include TILDE [Verdie et al., 2015] and LIFT [Yi et al., 2016]. TILDE [Verdie et al., 2015] generates the data set using patches with confident SIFT key points as positive samples and the ones far from key points as negative samples, and the regressor is a piece-wise linear function expressed via Generalized Hinging Hyperplanes (GHH). LIFT [Yi et al., 2016] takes an inverse order during the training process, first the local descriptor, then the orientation estimator and finally the detector. The orientation estimator is trained under constraints of the descriptors gained before. The detector is also a linear function of GHH, but adds one more constraint based on the orientation estimator and descriptor. One typical self-supervised method is SuperPoint [DeTone et al., 2018]. SuperPoint firstly generates simulated data like points and line segments with key point labels to train the MagicPoint, and the model is used to generate pseudo labels via homography adaption subsequently.

For the unsupervised methods, one idea is to use the repeatability of key points, like LF-Net [Ono et al., 2018], RF-Net [Shen et al., 2019], UnsuperPoint [Christiansen et al., 2019] and Key.Net [Barroso-Laguna et al., 2019], another idea is to utilize the local descriptors to drive the training process of the detector, like D2-Net [Dusmanu et al., 2019], R2D2 [Revaud et al., 2019] and ASLFeat [Luo et al., 2020]. Key.Net [Barroso-Laguna et al., 2019] proposes the index proposal (IP) layer based on softmax operation for location regression, and defines the MSE loss of correspondence location error weighted by corresponding responses. While LF-Net [Ono et al., 2018], RF-Net [Shen et al., 2019] and UnsuperPoint [Christiansen et al., 2019] use the MSE of responses as loss function instead. Actually, these approaches are usually not easy to train due to lack of strong constraints. Moreover, for training with MSE of responses, the detector is easy to be stuck into collapsed solution where all scores corresponding to each pixel are 0. Approaches like D2-Net [Dusmanu et al., 2019], R2D2 [Revaud et al., 2019] and ASLFeat [Luo et al., 2020] jointly train the descriptor and detector, where the detector and the descriptor are optimized via one shared loss function. Constructed based on convolution features with a shared loss function, from which the detector can derive semantic information. However, the information cannot guide fine location due to the expansion of receptive fields and loss of detailed information in the local features.

## 3 Approaches

### 3.1 Detector Structure

The structure of our guided local entropy optimal detector (GLEO-Det), is shown in Fig. 1 (a), consisting of three parts which are the backbone, the guider as well as the LEO-Det. In this paper, we use VGG-16 [Simonyan and Zisserman, 2014] as the backbone, where the former 4 blocks are used and the output feature map of each block is the input of the proposed LEO-Det. As for the specific architecture of the LEO-Det, we try UNet [Ronneberger et al., 2015] structure as shown in Fig. 1(b). In the Guider block, an extra convolution block is adopted to give a weight map, where Sigmoid operation is followed to ensure the weight map ranges from 0 to 1, indicating the importance of each output feature of the backbone. In the backbone of VGG-16, no normalization operation is needed, while in the Guider and the LEO-Det parts, the instance normalization [Ulyanov et al., 2016] is applied.

### 3.2 Local Entropy-based (LE) Loss

Current unsupervised pipelines usually optimize repeatability via MSE loss, which cannot provide enough constraint during the training process, and can be easily stuck into collapsed solution when MSE of responses are directly adopted. To address the issue, we use the local soft cross-entropy loss function for further learning when the response distributions for corresponding locations are the same. Using this approach, we only need one epoch with 2000 iterations for the detector training process, where one image is used in each iteration, showing the efficiency of our method.

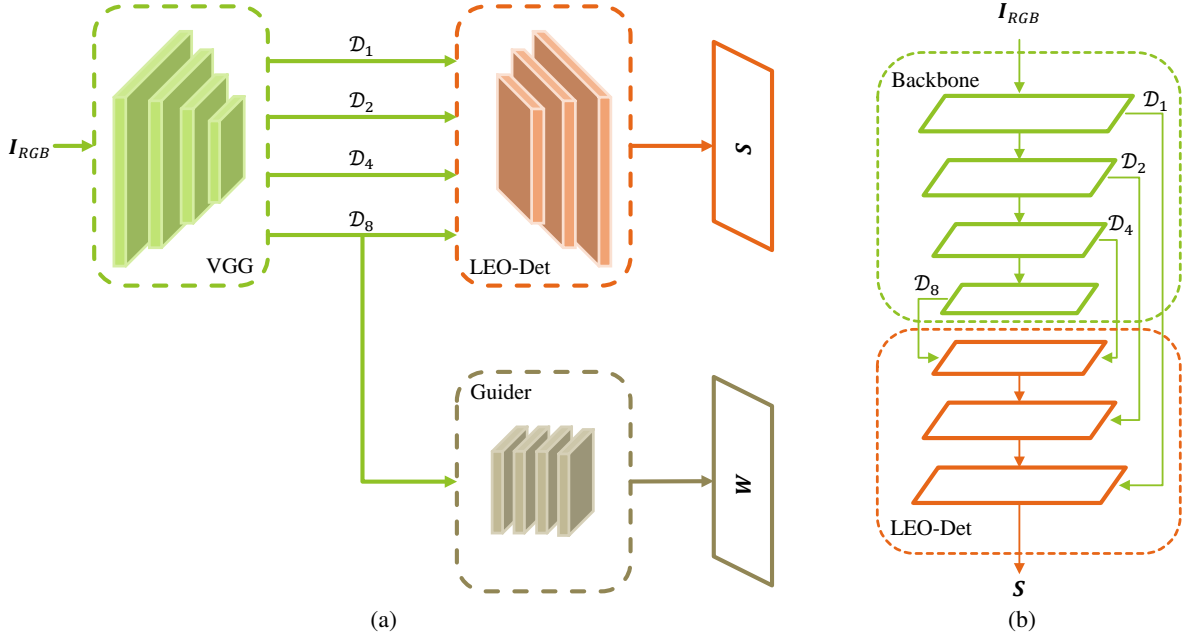


Figure 1: (a) shows the proposed pipeline to get the score map  $S$  and the weight map  $W$ , where  $D_k, k = 1, 2, 4, 8$  refers to the feature maps of different convolutional layers and  $k$  is the downsampling rate. For score map  $S$ , ReLU is used to make all elements positive and for the weight map  $W$ , sigmoid is adopted to ensure all values range from 0 to 1. (b) shows the UNet structures of the LEO-Det in this paper.

Suppose the response maps of images  $I_1$  and  $I_2$  with overlapped areas are denoted as  $S_1$  and  $S_2$ , where the ground true homography from  $I_1$  to  $I_2$  is  $H$  and the spatial mapping is  $t$ .

Assume that the size of both images are  $H \times W = 8w \times 8h$ . In this paper, like SuperPoint, we assume adopt the  $8 \times 8$  grid as a sample for loss function. With the ground true spatial mapping  $t$  from  $I_1$  to  $I_2$ , we have the aligned response map pairs  $(S_1, t^{-1}(S_2))$  and  $(t(S_1), S_2)$ . Then reshape them into 3D tensors denoted as  $(S_1, S_2^t)$  and  $(S_1^t, S_2)$ , which are all of  $64 \times w \times h$ . In this paper, we use the location with the highest score in each grid to select training samples. The feature point index matrices of  $I_1$  and  $I_2$  are written as,

$$\mathbf{K}_{1ij} = \arg \max_{1 \leq k \leq 64} S_{1kij}, \quad \mathbf{K}_{2ij} = \arg \max_{1 \leq k \leq 64} S_{2kij} \quad (1)$$

Then we select the indices in  $S_1$  and  $S_2$  to build set  $A$  defined as follow,

$$\begin{aligned} x_{ij} &= 8(j-1) + (\mathbf{K}_{1ij} \bmod 8), & y_{ij} &= 8(i-1) + \lfloor \mathbf{K}_{1ij}/8 \rfloor \\ p_{ij} &= 8(j-1) + (\mathbf{K}_{2ij} \bmod 8), & q_{ij} &= 8(i-1) + \lfloor \mathbf{K}_{2ij}/8 \rfloor \\ A &= \{(a, b, c, d) \mid \lfloor f(\mathbf{H}, [x_{ab}, y_{ab}]^T)/8 \rfloor = [c, d]^T \wedge \lfloor f(\mathbf{H}, [p_{cd}, q_{cd}]^T)/8 \rfloor = [a, b]^T\} \end{aligned} \quad (2)$$

Let  $[x', y', z'] = \mathbf{H}[x, y, 1]^T$ , then  $f$  is defined as,

$$f(\mathbf{H}, [x, y]^T) = [x'/z', y'/z']^T \quad (3)$$

To define the loss function, we write the slices of the tensors as,

$$\begin{aligned} \mathbf{u}_{ij} &= sm(S_{1:iij}), & \mathbf{u}'_{ij} &= sm(S_{1^t:iij}) \\ \mathbf{v}_{ij} &= sm(S_{2:ij}), & \mathbf{v}'_{ij} &= sm(S_{2^t:ij}) \end{aligned} \quad (4)$$

where  $sm$  refers to softmax operation and each element can be seen as the probability of the corresponding location to be a key point. The local similarity matrices can be defined in the form of cross-entropy as follow.

$$\begin{aligned} E_{1ij} &= - \sum_k (\mathbf{u}_{ijk} \log \mathbf{v}'_{ijk} + \mathbf{v}'_{ijk} \log \mathbf{u}_{ijk}) \\ E_{2ij} &= - \sum_k (\mathbf{v}_{ijk} \log \mathbf{u}'_{ijk} + \mathbf{u}'_{ijk} \log \mathbf{v}_{ijk}) \end{aligned} \quad (5)$$

For each  $\mathbf{x} = (a, b, c, d) \in A$ , let  $\mathbf{E}_{1\mathbf{x}} = \mathbf{E}_{1ab}$ ,  $\mathbf{E}_{2\mathbf{x}} = \mathbf{E}_{2cd}$ , and the LE loss is define below,

$$\mathcal{L}_{le} = \frac{1}{4|A|} \sum_{\mathbf{x} \in A} (\mathbf{E}_{1\mathbf{x}} + \mathbf{E}_{2\mathbf{x}}) \quad (6)$$

### 3.3 Guided Local Entropy-based (GLE) Loss

Guider is to point out the significant areas with salient features and smooth areas in the image and assign ballots for entropy-based loss of each local grid mentioned above. In addition, with the Guider, we can further force the energy of grids with key points to gather and that of smooth grids to scatter on the other side.

Suppose the weight maps output by Guider is denoted as  $\mathbf{W}_1$  and  $\mathbf{W}_2$  respectively. For each  $\mathbf{x} = (a, b, c, d) \in A$ , we let  $\mathbf{W}_{1\mathbf{x}} = \mathbf{W}_{1ab}$ ,  $\mathbf{W}_{2\mathbf{x}} = \mathbf{W}_{2cd}$ ,  $\mathbf{W}_{\mathbf{x}} = \mathbf{W}_{1\mathbf{x}}\mathbf{W}_{2\mathbf{x}}$ . With the weight maps, we can rewrite the LE loss as follow,

$$\mathcal{L}_{le}^W = \frac{1}{4 \sum_{\mathbf{x} \in A} \mathbf{W}_{\mathbf{x}}} \sum_{\mathbf{x} \in A} (\mathbf{E}_{1\mathbf{x}} + \mathbf{E}_{2\mathbf{x}}) \mathbf{W}_{\mathbf{x}} \quad (7)$$

For further improvement of the repeatability under more strict requirements, we add the term of certainty via self-information of each grid. In other words, grids with high weight should be more confident in key point location. Based on this, we use certainty matrices to depict the confidence of each grid.

$$\begin{aligned} \mathbf{C}_{1ij} &= - \sum_k (\mathbf{u}_{ijk} \log \mathbf{u}_{ijk} + \mathbf{v}'_{ijk} \log \mathbf{v}'_{ijk}) \\ \mathbf{C}_{2ij} &= - \sum_k (\mathbf{v}_{ijk} \log \mathbf{v}_{ijk} - \mathbf{u}'_{ijk} \log \mathbf{u}'_{ijk}) \end{aligned} \quad (8)$$

The local certainty loss, the other term of GLE loss, is

$$\mathcal{L}_{lc}^W = \frac{1}{4 \sum_{\mathbf{x} \in A} \mathbf{W}_{\mathbf{x}}} \sum_{\mathbf{x} \in A} (\mathbf{C}_{1\mathbf{x}} + \mathbf{C}_{2\mathbf{x}}) \mathbf{W}_{\mathbf{x}} - \frac{1}{4 \sum_{\mathbf{x} \in A} (1 - \mathbf{W}_{\mathbf{x}})} \sum_{\mathbf{x} \in A} (\mathbf{C}_{1\mathbf{x}} + \mathbf{C}_{2\mathbf{x}}) (1 - \mathbf{W}_{\mathbf{x}}) \quad (9)$$

where for each  $\mathbf{x} = (a, b, c, d) \in A$ ,  $\mathbf{C}_{1\mathbf{x}} = \mathbf{C}_{1ab}$ ,  $\mathbf{C}_{2\mathbf{x}} = \mathbf{C}_{2cd}$ .  $\mathcal{L}_{lc}^W$  not only requires the grids with high weights to be more certain for key point location, but also requires grids with low weights to be ambiguous on the other side. And the guided local entropy loss is a combination of both parts, which is,

$$\mathcal{L}_{gle} = \mathcal{L}_{le}^W + \mathcal{L}_{lc}^W \quad (10)$$

### 3.4 Inference

In this paper, we train our model using GLE loss function. With the score map  $\mathbf{S}$  output by the trained detector, we use the weight map  $\mathbf{W}$  of the Guider to remove the features that are not suitable for matching. Specifically, the weighted score map is written as follow,

$$\mathbf{S}_w = \text{Int}(\mathbf{W}) \odot \mathbf{S} \quad (11)$$

where  $\text{Int}$  refers to the bilinear interpolation operation and  $\odot$  is Hardmard product. In the validation stage, we choose the top  $k$  locations with the highest responses as key points for matching. In this paper, we take  $k = 3000$ .

### 3.5 Data set

In this paper, we adopt the Random Web Images in R2D2 to train our model, which contains 3125 images. To train the detector, random projection transform as well as color and contrast adjustments are used to construct image pairs with augmentation. Besides, the classic HPatches [Balntas et al., 2017] data set is used for validation. The data set contains 116 sequences, where each contains 6 images with the homography known between each other. HPatches data set involves two types of changes, including 59 sequences with *viewpoint* changes and 57 sequences with *illumination* changes.

## 4 Experiment

### 4.1 Ablation studies

In this part, we attempt to validate the effect of LE Loss and the GLE loss. To show that the entropy-based loss is more suitable for detector training, as a control group, we take the MSE loss to optimize the response map, and use the

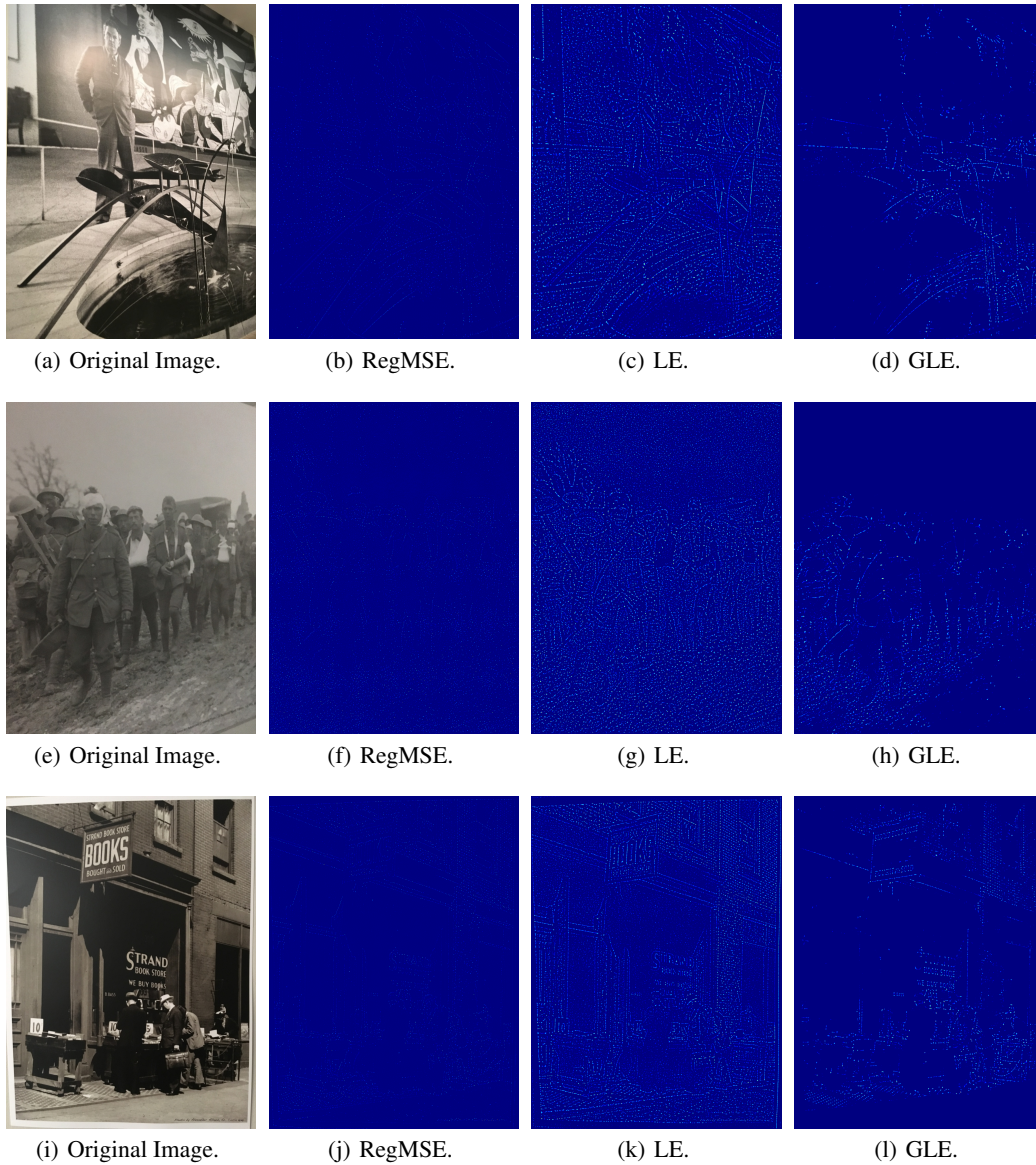


Figure 2: Score maps using different methods in Tab. 1, and we can see that the Guider module is essential in rejecting points with little semantic information.

Table 1: Ablation studies. The table shows the repeatability(Rep) and mean matching accuracy(MMA) at precision threshold  $\epsilon = 1$ . For evaluation with MMA, HardNet++(HN++) is used to construct descriptors. We denote the detector structure as  $F$  and test it trained with RegMSE, LE and GLE loss function respectively.

	HPatches <i>illu</i>		HPatches <i>view</i>		Overall	
	%rep@1	%mma@1	%rep@1	%mma@1	%rep@1	%mma@1
$F$ +RegMSE+HN++	37.16	59.03	19.96	25.34	28.41	41.56
$F$ +LE+HN++	42.56	61.93	30.27	31.82	36.31	46.32
$F$ +GLE+HN++	<b>48.43</b>	<b>69.07</b>	<b>42.84</b>	<b>37.73</b>	<b>45.58</b>	<b>52.82</b>

distance between the highest response and average response of the  $8 \times 8$  grid for regularization, which we name as regularized MSE (RegMSE). Furthermore, to verify that the Guider module is helpful for removing features without rich semantic information, we compare the performance of the detectors trained with  $\mathcal{L}_{le}$  in Eq. (6) and  $\mathcal{L}_{gle}$  in Eq. (10) respectively. For evaluation, we test the repeatability and mean matching accuracy (MMA) at error threshold  $\epsilon = 1$  which is a strict requirement on the HPatches with illumination changes as well as viewpoint changes. The results are shown in Tab. 1. In addition, we also show the score maps of one example using the above three methods in Fig. 2.

From Tab. 1 and the second column of Fig. 2, it can be seen that regularization does help for inhibiting possible collapsed solution. However, using local entropy-based loss function without Guider still performs better when precision requirement is quite strict, and this tells that entropy-based optimization is more suitable for detector training. Moreover, from Tab. 1, we can see that with the Guider block, training with GLE loss is better than only with LE loss and RegMSE. Combining with Fig. 2, we believe that is because the Guider module can help to reject the features with little semantic information.

Table 2: The table shows the repeatability of our method and other methods including typical handcrafted features, self-supervised learning based ones and unsupervised learning based ones. And we test the cases with the precision threshold  $\epsilon = 1$  and  $\epsilon = 3$ , which are rep@1 and rep@3 respectively. From the table, it can be seen that our approach performs the best when the precision requirements are more strict.

	HPatches <i>illu</i>		HPatches <i>view</i>		HPatches <i>Overall</i>	
	%rep@1	%rep@3	%rep@1	%rep@3	%rep@1	%rep@3
SIFT	25.15	43.89	24.90	52.16	25.02	48.10
SuperPoint	23.72	50.45	19.37	51.00	50.73	21.50
LF-Net	26.68	46.43	17.45	39.62	21.99	42.96
D2-Net	10.02	36.43	4.90	31.08	7.41	33.71
R2D2	31.32	63.65	27.46	63.21	29.36	63.43
ASLFeat	32.77	60.49	28.32	62.48	30.51	61.50
Key.Net	35.87	59.19	33.29	62.94	34.25	60.59
<i>F+GLE</i>	<b>48.43</b>	<b>61.64</b>	<b>42.84</b>	<b>64.87</b>	<b>45.58</b>	<b>64.28</b>

Table 3: The table compares our method to other methods including typical handcrafted features, self-supervised learning based ones and unsupervised learning based ones via MMA. And the precision threshold is  $\epsilon = 3$ . During comparison, we use HardNet++ to construct descriptors for all detectors and we can see that our approach performs the best.

	HPatches <i>illu</i>		HPatches <i>view</i>		HPatches <i>Overall</i>	
	%mma@1	%mma@3	%mma@1	%mma@3	%mma@1	%mma@3
SIFT	36.24	47.92	32.77	51.77	34.44	49.92
SuperPoint	43.01	69.38	25.50	59.88	33.93	64.46
LF-Net	37.87	57.31	24.02	49.02	30.69	53.01
D2-Net	19.37	50.21	6.48	31.62	12.69	40.57
R2D2	32.28	71.47	22.99	66.00	27.42	68.64
ASLFeat	46.92	77.45	33.18	67.44	39.79	72.26
Key.Net+HN++	43.32	72.31	33.24	<b>70.52</b>	38.09	71.38
<i>F+GLE+HN++</i>	<b>64.24</b>	<b>79.27</b>	<b>36.15</b>	67.41	<b>49.67</b>	<b>73.12</b>

## 4.2 Repeatability

In this part, we test the method on the entire HPatches, where our methods are compared with the other three types of methods. The first type is of the handcrafted feature detection methods including Harris, FAST as well as SIFT. The second type is of supervised/self-supervised like LIFT and SuperPoint. The third one is of unsupervised learning-based pipelines including LF-Net, RF-Net, Key.Net, D2-Net and ASLFeat. We test the repeatability of different methods with error threshold  $\epsilon$  of 1, 3 pixels respectively. Tab. 2 shows the average repeatability of each threshold on different validation set, including the HPatches with illumination changes, HPatches with viewpoint changes.

As shown in Tab. 2, our GLEO-Det has the best repeatability when  $\epsilon = 1$  and  $\epsilon = 3$ , showing that the GLEO-Det is stable for feature detection. Compared with D2-Net and ASLFeat, this demonstrates that our GLEO-Det can achieve fine constraint for the detector via local entropy taken into account. Moreover, we only train the detector using one

epoch with 2000 iterations. This shows that the loss function based on local entropy can facilitate the training process of the detector, make it more efficient.

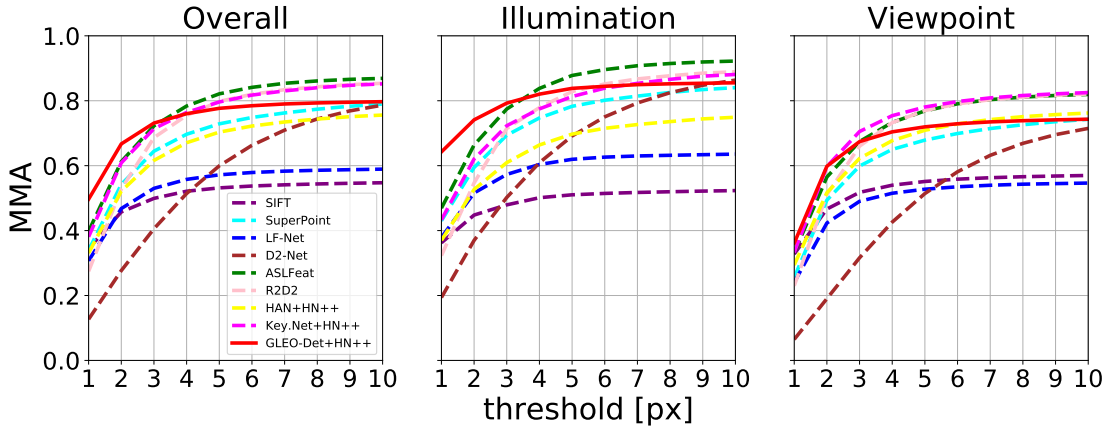


Figure 3: The MMA curves of the methods in Tab. 3 under different thresholds. From the figure we can see that our approach shows the best performance when the threshold is small. However, it can also be seen that our method is worse than R2D2, ASLFeat and Key.Net when threshold is larger especially for viewpoint change case, which is because we haven’t take scale factor into consideration and the performance of HN++ is limited.

### 4.3 Matchability

For testing, we remove 8 groups in HPatches as in D2-Net. In this paper, we use the mean matching accuracy (MMA) to evaluate the feature detection algorithms. We also include the three types of approaches above for evaluation. In addition, for correspondence establishment, we use HardNet (HN++) [Mishchuk et al., 2017] to build descriptors for the features and match through the nearest neighbor algorithm. The average MMA is shown in Tab. 3 and Fig. 3.

From Tab. 3 and Fig. 3, we can see that our GLEO-Det shows competitive performance using HardNet descriptors for matching, especially when the threshold is more strict. And this tells that the features detected using GLEO-Det are not only precisely repeatable but also stable for matching. On the other hand, it can also be seen that our method performs worse than R2D2, ASLFeat and Key.Net when threshold is larger especially for viewpoint change case. We believe one reason is that we haven’t taken scale factor into consideration as Key.Net and directly crop  $32 \times 32$  patches surrounding key points for descriptor construction. The other reason is that the performance of HN++ is limited in certain degree.

## 5 Conclusion

In this paper, we propose an unsupervised pipeline for feature detection in images. Specifically, we attempt to combine the repeatability requirement and convolution feature guidance for better performance. In addition, entropy-based object function is developed to make it more easier to reach convergence. Finally, with the Guider block, we define the loss function from two sides, both positive and negative, in order to remove the points with little semantic information. However, the matching performance is still limited to the descriptors. Therefore, in our future work, we will attempt to establish guiding mechanism from detector to descriptor, and achieve mutual learning between both detector and descriptor.

## References

- Chris Harris, Mike Stephens, et al. A combined corner and edge detector. In *Alvey vision conference*, volume 15, pages 10–5244. Citeseer, 1988.
- Stephen M Smith and J Michael Brady. Susan—a new approach to low level image processing. *International journal of computer vision*, 23(1):45–78, 1997.
- Miroslav Trajković and Mark Hedley. Fast corner detection. *Image and vision computing*, 16(2):75–87, 1998.
- Ethan Rublee, Vincent Rabaud, Kurt Konolige, and Gary Bradski. Orb: An efficient alternative to sift or surf. In *2011 International conference on computer vision*, pages 2564–2571. Ieee, 2011.



- Elmar Mair, Gregory D Hager, Darius Burschka, Michael Suppa, and Gerhard Hirzinger. Adaptive and generic corner detection based on the accelerated segment test. In *European conference on Computer vision*, pages 183–196. Springer, 2010.
- Tony Lindeberg. Feature detection with automatic scale selection. *International journal of computer vision*, 30(2): 79–116, 1998.
- David G Lowe. Object recognition from local scale-invariant features. In *Proceedings of the seventh IEEE international conference on computer vision*, volume 2, pages 1150–1157. Ieee, 1999.
- David G Lowe. Distinctive image features from scale-invariant keypoints. *International journal of computer vision*, 60(2):91–110, 2004.
- Herbert Bay, Tinne Tuytelaars, and Luc Van Gool. Surf: Speeded up robust features. In *European conference on computer vision*, pages 404–417. Springer, 2006.
- Jiri Matas, Ondrej Chum, Martin Urban, and Tomas Pajdla. Robust wide-baseline stereo from maximally stable extremal regions. *Image and vision computing*, 22(10):761–767, 2004.
- Yann LeCun, Leon Bottou, Yoshua Bengio, and Patrick Haffner. Gradient-based learning applied to document recognition. *Proceedings of the IEEE*, 86(11):2278–2324, 1998.
- Kwang Moo Yi, Eduard Trulls, Vincent Lepetit, and Pascal Fua. Lift: Learned invariant feature transform. In *European conference on computer vision*, pages 467–483. Springer, 2016.
- Yannick Verdie, Kwang Yi, Pascal Fua, and Vincent Lepetit. Tilde: A temporally invariant learned detector. In *Proceedings of the IEEE conference on computer vision and pattern recognition*, pages 5279–5288, 2015.
- Daniel DeTone, Tomasz Malisiewicz, and Andrew Rabinovich. Superpoint: Self-supervised interest point detection and description. In *Proceedings of the IEEE conference on computer vision and pattern recognition workshops*, pages 224–236, 2018.
- Yuki Ono, Eduard Trulls, Pascal Fua, and Kwang Moo Yi. Lf-net: Learning local features from images. *Advances in neural information processing systems*, 31, 2018.
- Xuelun Shen, Cheng Wang, Xin Li, Zenglei Yu, Jonathan Li, Chenglu Wen, Ming Cheng, and Zijian He. Rf-net: An end-to-end image matching network based on receptive field. In *Proceedings of the IEEE/CVF Conference on Computer Vision and Pattern Recognition*, pages 8132–8140, 2019.
- Peter Hviid Christiansen, Mikkel Fly Kragh, Yury Brodskiy, and Henrik Karstoft. Unsuperpoint: End-to-end unsupervised interest point detector and descriptor. *arXiv preprint arXiv:1907.04011*, 2019.
- Axel Barroso-Laguna, Edgar Riba, Daniel Ponsa, and Krystian Mikolajczyk. Key. net: Keypoint detection by handcrafted and learned cnn filters. In *Proceedings of the IEEE/CVF International Conference on Computer Vision*, pages 5836–5844, 2019.
- Mihai Dusmanu, Ignacio Rocco, Tomas Pajdla, Marc Pollefeys, Josef Sivic, Akihiko Torii, and Torsten Sattler. D2-net: A trainable cnn for joint description and detection of local features. In *Proceedings of the IEEE/cvf conference on computer vision and pattern recognition*, pages 8092–8101, 2019.
- Jerome Revaud, Philippe Weinzaepfel, Cesar De Souza, Noe Pion, Gabriela Csurka, Johann Cabon, and Martin Humenberger. R2d2: repeatable and reliable detector and descriptor. *arXiv preprint arXiv:1906.06195*, 2019.
- Zixin Luo, Lei Zhou, Xuyang Bai, Hongkai Chen, Jiahui Zhang, Yao Yao, Shiwei Li, Tian Fang, and Long Quan. Aslfeat: Learning local features of accurate shape and localization. In *Proceedings of the IEEE/CVF conference on computer vision and pattern recognition*, pages 6589–6598, 2020.
- Karen Simonyan and Andrew Zisserman. Very deep convolutional networks for large-scale image recognition. *arXiv preprint arXiv:1409.1556*, 2014.
- Olaf Ronneberger, Philipp Fischer, and Thomas Brox. U-net: Convolutional networks for biomedical image segmentation. In *International Conference on Medical image computing and computer-assisted intervention*, pages 234–241. Springer, 2015.
- Dmitry Ulyanov, Andrea Vedaldi, and Victor Lempitsky. Instance normalization: The missing ingredient for fast stylization. *arXiv preprint arXiv:1607.08022*, 2016.
- Vassileios Balntas, Karel Lenc, Andrea Vedaldi, and Krystian Mikolajczyk. Hpatches: A benchmark and evaluation of handcrafted and learned local descriptors. In *Proceedings of the IEEE conference on computer vision and pattern recognition*, pages 5173–5182, 2017.
- Anastasiia Mishchuk, Dmytro Mishkin, Filip Radenovic, and Jiri Matas. Working hard to know your neighbor’s margins: Local descriptor learning loss. *Advances in neural information processing systems*, 30, 2017.